ASSOCIAÇÃO BRASILEIRA DE ENERGIA NUCLEAR - ABEN
2019 International Nuclear Atlantic Conference - INAC 2019
Santos, SP, Brazil, October 21-25, 2019

Agência Brasileira do ISBN
ISBN 978-85-99141-08-3
9 788599 141083

THE SPECTRAL DETERMINISTIC METHOD APPLIED TO NEUTRON FIXED-SOURCE DISCRETE ORDINATES PROBLEMS IN X, Y-GEOMETRY FOR MULTIGROUP CALCULATIONS

Amaury Muñoz Oliva[1], Hermes Alves Filho[2], Ricardo C. Barros[2] and Jesús Pérez Curbelo[2]

[1]Instituto de Pesquisas Energéticas e Nucleares (IPEN/CNEN)
Av. Professor Lineu Prestes 2242
05508-000 São Paulo, SP
amaury.oliva@ipen.br

[2]Departamento de Modelagem Computacional, Instituto Politécnico
Universidade do Estado do Rio de Janeiro
Rua Alberto Rangel, s/n
28630-050 Nova Friburgo, RJ
halves@iprj.uerj.br
rcbarros@pq.cnpq.br
jperez@iprj.uerj.br

ABSTRACT

A new approach for the development of a coarse-mesh numerical spectral nodal method is presented in this paper. This method, referred to as the Spectral Deterministic Method – Constant Nodal (*SDM–CN*), is based on a spectral analysis of the multigroup X,Y-Geometry, linearly anisotropic scattering neutron transport equations in discrete ordinates (S_N)formulation for fixed-source calculations in non-multiplying media. In this paper we present typical model problems to illustrate the accuracy and the efficiency for coarse-mesh energy multigroup S_N calculations of the *SDM-CN* method. The numerical results obtained are compared with the traditional fine-mesh Diamond Difference (*DD*) method and the results obtained by DOT–II and TWOTRAN codes. The numerical results are also compared with the spectral nodal method, spectral Green's function (*SGF*).

1. INTRODUCTION

The computational neutronic modeling within nuclear reactor engineering, has made a significant contribution to new nuclear projects. Developing codes and calculation models this modeling allows an accurate description of the neutron dynamics and thermohydraulic behavior of the current and future nuclear reactors, since they allow to simulate some processes that take place at the reactor's operation. It also has applications in radiation protection, agriculture, industry, nuclear medicine, making an essential economy and guaranteeing the safety of the installations through the use of simulators built by using high-performance programming languages.

The description of the neutron migration through a host medium, with the probability of interaction with the nuclei of the atoms of this medium, constitutes the physical modeling of the neutron transport phenomenon [1]. Once the physical modeling is done, it is performed the mathematical modeling of the problem to be able to simulate the neutron

distribution within the region of the physical space where it must analyze the neutron behavior. To made the mathematical modeling, is used the linear Boltzmann equation [2], that represents a balance between the production and loss of these particles, and in its generality, a partial integral-differential equation dependent on seven independent variables: three spatial, two angular, the particle energy, and time.

Due to the complexity in the analytical treatment to find a solution for the linear neutron transport equation, numerical methods have been developed to obtain approximate solutions for the neutron shielding problem and global nuclear reactor calculations. These numerical methods allows to make computational modeling using a deterministic approach. Generally, these methods use the discrete ordinates formulation S_N [2]. The S_N formulation made a collocation scheme for the angular variables in prescribed directions (discrete ordinates) and use an angular quadrature set for the approximation of the integral source terms [3].

This paper is organized as follows: Section 2. presents the spectral analysis of multigroup transport equations in discrete ordinates formulation. In Section 3., is described the iterative methodology of the multigroup Spectral Deterministic Method – Constant Nodal ($SDM - CN$) in X, Y– geometry geometry. Numerical results for one and two groups linearly anisotropic scattering S_N problems are given in Section 4. A brief discussion of the results and suggestions for future work are presented in Section 5.

2. MATHEMATICAL PRELIMINARIES

Considering the S_N equations in a rectangular domain D of width X and height Y with linearly anisotropic scattering:

$$\mu_m \frac{\partial}{\partial x}\psi_{m,g}(x,y)+\eta_m \frac{\partial}{\partial y}\psi_{m,g}(x,y)+\sigma_{T_g}(x,y)\psi_{m,g}(x,y) = \frac{1}{4}\sum_{g'=1}^{G}\{\sigma^{(0)}_{s_{g'\to g}}(x,y)\sum_{n=1}^{M}\psi_{n,g'}(x,y)\omega_n+$$
$$3\sigma^{(1)}_{s_{g'\to g}}(x,y)\mu_m\sum_{n=1}^{M}\mu_n\psi_{n,g'}(x,y)\omega_n + 3\sigma^{(1)}_{s_{g'\to g}}(x,y)\eta_m\sum_{n=1}^{M}\eta_n\psi_{n,g'}(x,y)\omega_n\} + Q_g(x,y),$$
$$g = 1:G,\ m = 1:M. \quad (1)$$

For each region analyzed in D, the term $\sigma_{T_g}(x,y)$, describe the g-th group macroscopic total cross section, $\sigma^{(0)}_{s_{g'\to g}}(x,y)$, represents the zero'th component of the macroscopic g-th isotropic differential scattering cross section from group g' to group g, $\sigma^{(1)}_{s_{g'\to g}}(x,y)$, is the first–order component of the macroscopic g-th isotropic differential scattering cross section from group g' to group g and $Q_g(x,y)$, represent the isotropic neutron source in energy group g. It is assumed that these quantities are piecewise constant functions in D [4].

In Eq.1 are considered as isotropic prescribed boundary conditions of the domain those

represented in the form

$$\begin{aligned}
\psi_g(0,y) &= p_g(y)\,, \quad \mu_m > 0,\\
\psi_g(X,y) &= q_g(y)\,, \quad \mu_m < 0,\\
\psi_g(x,0) &= u_g(x)\,, \quad \eta_m > 0,\\
\psi_g(x,Y) &= v_g(x)\,, \quad \eta_m < 0.
\end{aligned} \tag{2}$$

The quantities M represents the total number of discrete directions, which for the x, y geometry case, is calculated by the expression

$$M = \frac{N(N+2)}{2}\,, \tag{3}$$

N is the S_N quadrature order. In this work we use the quadrature level LQ_N (*Level Symmetric Quadrature*) [2], where ω_m are the weights of the angular quadrature associated to the discrete directions represented by the pair (μ_m, η_m),

Now we consider an arbitrary spatial grid on the domain D, as shown in Fig.1, where each spatial cell Γ_j have width h_{x_i} and height h_{y_j}, constant cross sections $\sigma^{(0)ij}_{s_{g'\to g}}$, $\sigma^{(1)ij}_{s_{g'\to g}}$, $\sigma^{ij}_{T_g}$ and constant interior source Q^{ij}_g .

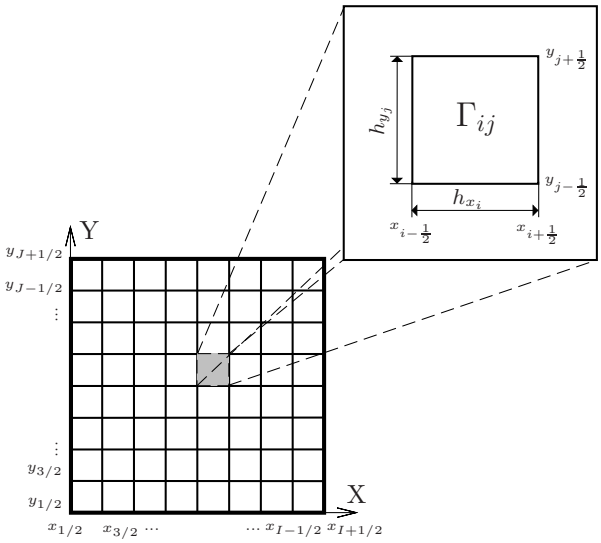

Figure 1: Discretization of the two-dimensional domain D in $I \times J$ spatial cells Γ_{ij} of width h_{x_i} and height h_{y_j}.

In order to obtain the one-dimensional transverse - integrated S_N nodal equations with linearly anisotropic scattering, the transverse-integration operators, are defined

$$\frac{1}{h_{u_s}} \int_{u_{s-\frac{1}{2}}}^{u_{s+\frac{1}{2}}} (\cdot) du\ , \tag{4}$$

where $u = x$ (or y) and $s = i$ (or j).

At first we choose to integrate Equation (1) in the y direction, where $u = y$ and $s = j$, to obtain the one-dimensional transverse-integrated S_N nodal equation for the x direction

$$\mu_m \frac{d}{dx}\widetilde{\psi}^{j}_{m,g}(x) + \frac{\eta_m}{h_{y_j}}\left(\psi^{j+\frac{1}{2}}_{m,g}(x) - \psi^{j-\frac{1}{2}}_{m,g}(x)\right) + \sigma^{ij}_{T_g}\widetilde{\psi}^{j}_{m,g}(x) = \frac{1}{4}\sum_{g'=1}^{G}\{\sigma^{(0)\,ij}_{s_{g'\to g}}\sum_{n=1}^{M}\widetilde{\psi}^{j}_{n,g'}(x)\omega_n$$
$$+ 3\sigma^{(1)\,ij}_{s_{g'\to g}}\mu_m\sum_{n=1}^{M}\mu_n\widetilde{\psi}^{j}_{n,g'}\omega_n + 3\sigma^{(1)\,ij}_{s_{g'\to g}}\eta_m\sum_{n=1}^{M}\eta_n\widetilde{\psi}^{j}_{n,g'}(x)\omega_n\} + Q^{ij}_{g} \quad ,$$
$$x \in \Gamma_{ij}, \quad i = 1:I, \quad j = 1:J, \quad \mathrm{m} = 1:\mathrm{M}, \quad g = 1:\mathrm{G} \ . \quad (5)$$

Similarly, is applied the operator (4) to Eq. (1) considering $u = x$ and $s = i$ and Eq. (1)is integrated over x to obtain the one-dimensional transverse-integrated S_N nodal equation for the y direction

$$\frac{\mu_m}{h_{x_i}}\left(\psi^{i+\frac{1}{2}}_{m,g}(y) - \psi^{i-\frac{1}{2}}_{m,g}(y)\right) + \eta_m\frac{d}{dy}\widehat{\psi}^{i}_{m,g}(y) + \sigma^{ij}_{T_g}\widehat{\psi}^{i}_{m,g}(y) = \frac{1}{4}\sum_{g'=1}^{G}\{\sigma^{(0)\,ij}_{s_{g'\to g}}\sum_{n=1}^{M}\widehat{\psi}^{i}_{n,g'}(y)\omega_n$$
$$+ 3\sigma^{(1)\,ij}_{s1_{g'\to g}}\mu_m\sum_{n=1}^{M}\mu_n\widehat{\psi}^{i}_{n,g'}(y)\omega_n + 3\sigma^{(1)\,ij}_{s_{g'\to g}}\eta_m\sum_{n=1}^{M}\eta_n\widehat{\psi}^{i}_{n,g'}(y)\omega_n\} + Q^{ij}_{g} \quad ,$$
$$y \in \Gamma_{ij}, \quad i = 1:I, \quad j = 1:J, \quad \mathrm{m} = 1:\mathrm{M}, \quad g = 1:\mathrm{G} \ , \quad (6)$$

where the group mean angular fluxes in each coordinate direction inside the $\Gamma_{i\,j}$ node are defined by

$$\widetilde{\psi}^{j}_{m,g}(x) = \frac{1}{h_{y_j}}\int_{y_{j-\frac{1}{2}}}^{y_{j+\frac{1}{2}}}\psi_{m,g}(x,y)\,dy \quad (7)$$

and

$$\widehat{\psi}^{i}_{m,\,g}(y) = \frac{1}{h_{x_i}}\int_{x_{i-\frac{1}{2}}}^{x_{i+\frac{1}{2}}}\psi_{m,\,g}(x,y)\,dx \ . \quad (8)$$

The equations (5) and (6) represent two systems of GM ordinary differential equations in coordinate directions x and y, respectively. Each system has $2GM$ unknowns, GM unknowns represented by $\widetilde{\psi}^{j}_{m,g}(x)$ (or $\widehat{\psi}^{i}_{m,g}(y)$) and GM unknowns represented by the transverse leakage terms. We assume that these transverse leakage terms are constant along the edges in each $\Gamma_{i\,j}$ nodes, constituting the only approximation performed at calculations in this work [5] [6]. Then, these transverse leakage terms approximation are presented as

$$\frac{\eta_m}{h_{y_j}}\left(\psi^{j+\frac{1}{2}}_{m,g}(x) - \psi^{j-\frac{1}{2}}_{m,g}(x)\right) \quad (9)$$

and

$$\frac{\mu_m}{h_{x_i}}\left(\psi^{i+\frac{1}{2}}_{m,g}(y) - \psi^{i-\frac{1}{2}}_{m,g}(y)\right) \ . \quad (10)$$

Considering this, it is assumed that these constants correspond to the mean values of the angular fluxes along the sides of the analyzed node, therefore

$$\psi^{j\pm\frac{1}{2}}_{m,g}(x) \approx \widehat{\psi}^{i,j\pm\frac{1}{2}}_{m,g} \quad (11)$$

and

$$\psi_{m,g}^{i\pm\frac{1}{2}}(y) \approx \widetilde{\psi}_{m,g}^{i\pm\frac{1}{2},j} \quad . \tag{12}$$

After assuming these approximations, the terms of transverse leakage can be defined as

$$\frac{\eta_m}{h_{y_j}}\left(\widehat{\psi}_{m,g}^{i,j+\frac{1}{2}} - \widehat{\psi}_{m,g}^{i,j-\frac{1}{2}}\right) \;=\; \widehat{L}_{m,g}^{i,j}\,, \tag{13}$$

and

$$\frac{\mu_m}{h_{x_i}}\left(\widetilde{\psi}_{m,g}^{i+\frac{1}{2},j} - \widetilde{\psi}_{m,g}^{i-\frac{1}{2},j}\right) \;=\; \widetilde{L}_{m,g}^{i,j}\,. \tag{14}$$

Consider constant approximations for the transverse leakage terms, the objective is to ensure the uniqueness for the solution of the transversally integrated S_N equations within each spatial discretization node, Γ_{ij}, with the boundary conditions and the conditions of continuity at the interfaces of the nodes. In other words, obtain two systems with GM equations and GM unknowns, coupled by the transverse leakage terms [6][8]. The constants to approximate these terms are chosen conveniently because it is desired to preserve the average fluxes on the sides of the node Γ_{ij}. Therefore, using the definitions (6) and (14) in Equations (5) and (6), we can rewrite the transversely integrated equations S_N in the form

$$\begin{aligned}\mu_m\frac{d}{dx}\widetilde{\psi}_{m,g}^{j}(x) + \widehat{L}_{m,g}^{i,j} + \sigma_{T_g}^{ij}\widetilde{\psi}_{m,g}^{j}(x) = \frac{1}{4}\sum_{g'=1}^{G}\{\sigma_{s_{g'\to g}}^{(0)\,ij}\sum_{n=1}^{M}\widetilde{\psi}_{n,g'}^{j}(x)\omega_n \\ + 3\sigma_{s_{g'\to g}}^{(1)\,ij}\mu_m\sum_{n=1}^{M}\mu_n\widetilde{\psi}_{n,g'}^{j}\omega_n + 3\sigma_{s_{g'\to g}}^{(1)\,ij}\eta_m\sum_{n=1}^{M}\eta_n\widetilde{\psi}_{n,g'}^{j}(x)\omega_n\} + Q_g^{ij}\ ,\quad , \\ x\in\Gamma_{ij},\quad i=1:I,\quad j=1:J,\quad \mathrm{m}=1:\mathrm{M},\quad g=1:\mathrm{G}\ .\end{aligned} \tag{15}$$

and

$$\begin{aligned}\widetilde{L}_{m,g}^{i,j} + \eta_m\frac{d}{dy}\widehat{\psi}_{m,i}(y) + \sigma_{T_g}^{ij}\widehat{\psi}_{m,i}(y) = \frac{1}{4}\sum_{g'=1}^{G}\{\sigma_{s_{g'\to g}}^{(0)\,ij}\sum_{n=1}^{M}\widehat{\psi}_{n,g'}^{i}(y)\omega_n \\ + 3\sigma_{s_{g'\to g}}^{(1)\,ij}\mu_m\sum_{n=1}^{M}\mu_n\widehat{\psi}_{n,g'}^{i}(y)\omega_n + 3\sigma_{s_{g'\to g}}^{(1)\,ij}\eta_m\sum_{n=1}^{M}\eta_n\widehat{\psi}_{n,g'}^{i}(y)\omega_n\} + Q_g^{ij}\ \ , \\ y\in\Gamma_{ij},\quad i=1:I,\quad j=1:J,\quad \mathrm{m}=1:\mathrm{M},\quad g=1:\mathrm{G}\ .\end{aligned} \tag{16}$$

The equations systems (15) and (16), considering a $X,Y-$ geometry domain, with uniform physical material parameters in each Γ_{ij} node to be analyzed, have a general solution, in the form

$$\widetilde{\psi}_{m,g}(x) = \widetilde{\psi}_{m,g}^{h}(x) + \widetilde{\psi}_{m,g}^{p}\,,\ x\in\Gamma_{ij}\ , \tag{17}$$

for the equation system (15), and

$$\widehat{\psi}_{m,g}(y) = \widehat{\psi}_{m,g}^{h}(y) + \widehat{\psi}_{m,g}^{p}\,,\ y\in\Gamma_{ij}\ , \tag{18}$$

Here the superscript p indicates the particular solution that is spatially constant in D and the superscript h indicates the homogeneous component of the solution, which satisfies the homogeneous equation associated with Eqs. (15) and (16). In order to determine

the particular solution of the system (15), the fluxes $\widetilde{\psi}^{j}_{m,g}(x)$ are substituted for $\widetilde{\psi}^{p}_{m,g}$, obtaining

$$\frac{1}{4}\sum_{g'=1}^{G}\sum_{n=1}^{M}\left(4\sigma^{ij}_{T_g}\delta_{mn}\delta_{g'g}-\left[\sigma^{(0)\,ij}_{s_{g'\to g}}+3\sigma^{(1)\,ij}_{s_{g'\to g}}\{\mu_m\mu_n+\eta_m\eta_n\}\right]\omega_n\right)\widetilde{\psi}^{p}_{n,\,g'}=Q^{ij}_{g}-\widehat{L}^{i,j}_{m,g}\quad,$$
$$\mathrm{m}=1:\mathrm{M},\quad g=1:\mathrm{G}\ . \tag{19}$$

$$\text{where }\ \delta_{a,b}=\begin{cases}1 & \text{para}\quad a=b\\ 0 & \text{para}\quad a\neq b\end{cases}\ \text{, represents the } \textit{Krönecker delta.}$$

Doing the same analysis for the system given in Equation (16), it is obtained

$$\frac{1}{4}\sum_{g'=1}^{G}\sum_{n=1}^{M}\left(4\sigma^{ij}_{T_g}\delta_{mn}\delta_{g'g}-\left[\sigma^{(0)\,ij}_{s_{g'\to g}}+3\sigma^{(1)\,ij}_{s_{g'\to g}}\{\mu_m\mu_n+\eta_m\eta_n\}\right]\omega_n\right)\widehat{\psi}^{p}_{n,\,g'}=Q^{ij}_{g}-\widetilde{L}^{i,j}_{m,g}\quad,$$
$$\mathrm{m}=1:\mathrm{M},\quad g=1:\mathrm{G}\ . \tag{20}$$

The homogeneous solution of Equation (15) has the form

$$\widetilde{\psi}^{hj}_{m,g}(x)=a^{x}_{m,g}(\nu^x)e^{\dfrac{-\left(x-x_{j-\frac{1}{2}}\right)}{\nu^x}}\quad,\quad m=1:\mathrm{M},\quad x\in\Gamma_{\mathrm{i}}\mathrm{j}\ , \tag{21}$$

Substituting the equation (21) into the homogeneous part of Equation (15), considering the source $Q^{ij}_{g}=0$ and $\widehat{L}^{i,j}_{m,g}=0$, is obtained

$$\frac{1}{4\mu_m}\sum_{g'=1}^{G}\sum_{n=1}^{M}\left(4\sigma^{ij}_{T_g}\delta_{g'g}\delta_{mn}-\left[\sigma^{(0)\,ij}_{s_{g'\to g}}+3\sigma^{(1)\,ij}_{s_{g'\to g}}\{\mu_m\mu_n+\eta_m\eta_n\}\right]\omega_n\right)a^{x}_{n,g'}(\nu^x)\ =$$
$$\frac{1}{\nu^x}a^{x}_{m,g}(\nu^x)\quad,$$
$$\mathrm{m}=1:\mathrm{M},\quad g=1:\mathrm{G}\ . \tag{22}$$

A procedure analogous to that done for Equation (15), can be performed to solve the system of equations (16), considering for this case $\widetilde{L}^{i,j}_{m,g}=0$, obtaining the system of equations

$$\frac{1}{4\eta_m}\sum_{g'=1}^{G}\sum_{n=1}^{M}\left(4\sigma^{ij}_{T_g}\delta_{g'g}\delta_{mn}-\left[\sigma^{(0)\,ij}_{s_{g'\to g}}+3\sigma^{(1)\,ij}_{s_{g'\to g}}\{\mu_m\mu_n+\eta_m\eta_n\}\right]\omega_n\right)a^{y}_{n,\,g'}(\nu^y)\ =$$
$$\frac{1}{\nu^y}a^{y}_{m,g}(\nu^y)\quad,$$
$$\mathrm{m}=1:\mathrm{M},\quad g=1:\mathrm{G}\ . \tag{23}$$

Both equations (22) and (23), in a matrix notation, can be written in the form

$$A\mathbf{a}=\frac{1}{\nu}\mathbf{a}, \tag{24}$$

where, similar to the one-dimensional case [3], A is a square real matrix, of order $GM\times GM$, and the eigenvalues ν^x and ν^y are all symmetric and appear in pairs of opposite signs, due to the symmetry of angular quadrature used.

Therefore, the local general solution for each S_N equations system within each nodeΓ_{ij}, (15) and (16), respectively, appear in the form

$$\widetilde{\psi}^{j}_{m,g}(x) = \sum_{\ell=1}^{GM} \alpha^{x}_{\ell}\, a^{x}_{m,g}(\nu^{x}_{\ell})\, e^{\dfrac{-\left(x - x_{i-\frac{1}{2}}\right)}{\nu^{x}_{\ell}}} + \widetilde{\psi}^{p}_{m,g}\ , \quad m = 1:\mathrm{M}, \quad g = 1:\mathrm{G}, \quad x \in \Gamma_{\mathrm{ij}} \tag{25}$$

and

$$\widehat{\psi}^{i}_{m,g}(y) = \sum_{\ell=1}^{GM} \alpha^{y}_{\ell}\, a^{y}_{m,g}(\nu^{y}_{\ell})\, e^{\dfrac{-\left(y - y_{j-\frac{1}{2}}\right)}{\nu^{y}_{\ell}}} + \widehat{\psi}^{p}_{m,g}\ , \quad m = 1:\mathrm{M}, \quad g = 1:\mathrm{G}, \quad y \in \Gamma_{\mathrm{ij}}\,, \tag{26}$$

where the parameters α^{x}_{ℓ} and α^{y}_{ℓ} are arbitrary constants to be determined according to the boundary conditions of the spatial discretization node.

3. THE MULTIGROUP SPECTRAL DETERMINISTIC METHOD–CONSTANT NODAL(SDM–CN)

In this section it is described the iterative process for solving the $SDM - CN$ neutron transport equation, spatially and angularly discretized in the multigroup formulation.

After obtaining the α^{x}_{ℓ} and α^{y}_{ℓ} parameters, the outgoing fluxes of the analyzed node are computed using the same equations, (25) and (26). Then, the α_{ℓ} parameters and the outgoing fluxes at each spatial node's output are calculated using Eqs.(25) and (26). Reached this point, it becomes necessary to define the concept of sweeping the spatial discretization X, Y– geometry grid, to understand the dynamics of calculating the outgoing angular fluxes in the $SDM - CN$ iterative scheme. Similarly to the iterative algorithm of the SDM method for one-dimensional problems [3], the iterative algorithm for the X, Y– geometry case is essentially different from the transport sweeps employed by the methods DD [2] and SGF [9].

By defining the sweeping concept for a X, Y– geometry spatial discretization grid, Figure 1, using the SDM method, the coordinate system in Cartesian plane is initially taken as reference. The coordinate axes $(\mu_m; \eta_m)$ are oriented in the directions of $(x; y)$ respectively. Both axes range from negative to positive in the Cartesian coordinate system.

The numerical iterative process [7] is initiated by performing the spectral analysis of Equations (5) and (6) at the chosen node to start the sweeping process. This node $\Gamma_{i,j}$ can be located on the first or last row of the spatial discretization grid by combining it with the first or last column of the same grid. For this paper, we establish the starting node at the combination, first bottom row with first column on the left side, Figure 2. Once obtained the $a^{x}_{m,g}(\nu^{x}_{\ell})$ and $a^{y}_{m,g}(\nu^{y}_{\ell})$ eigenvectors with the corresponding eigenvalues ν_{ℓ} together with the particular solutions $\widetilde{\psi}^{p}_{n,g}$ and $\widehat{\psi}^{p}_{n,g}$ we proceed with the calculation of the α^{x}_{ℓ} and α^{y}_{ℓ} parameters at the first node $\Gamma_{i,j}$ using the Equations (25) and (26)

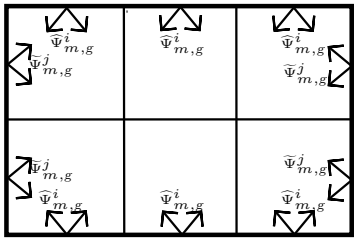

Figure 2: Bidimensional spatial grid with $\Gamma_{i,j}$ nodes, where $i = 1 : I$ e $j = 1 : J$

together with the pre-established boundary conditions on the left and lower sides of the node. For the incoming angular fluxes on the upper and right interfaces of the analyzed node, an initial estimate is made. Obtained the α_ℓ^x and α_ℓ^y parameters at the first node, using again the Equations (25) and (26), it can be determined the outgoing angular fluxes of first node in all energy groups.

Figure 3: Incomming and Outgoing angular fluxes of the node $\Gamma_{1,1}$ node

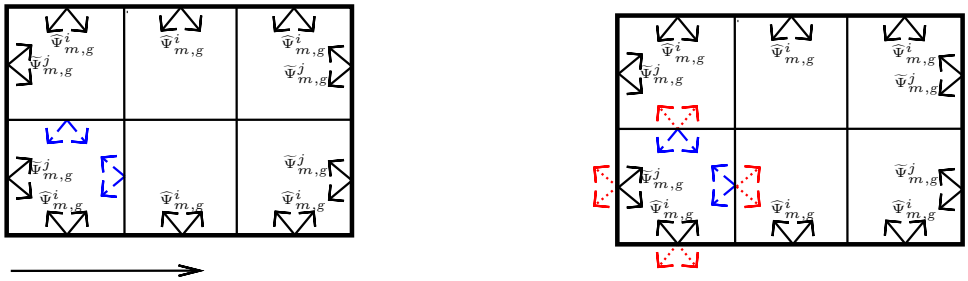

(a) Initial estimate

(b) Outgoing fluxes

Advancing to the right of the starting node, applying the continuity conditions we can use the outgoing angular fluxes in all energy groups in the right interface of this node as initial approximation for the incoming angular fluxes for the left side of the adjacent node. In the adjacent node, the incoming angular fluxes on the right and top interfaces continue as initial approximations. With the approximation of the incoming angular fluxes on the node, it is possible to calculate the α_ℓ parameters and the outgoing angular fluxes.

Figure 4: Incomming and Outgoing angular fluxes of the node $\Gamma_{i+1,1}$

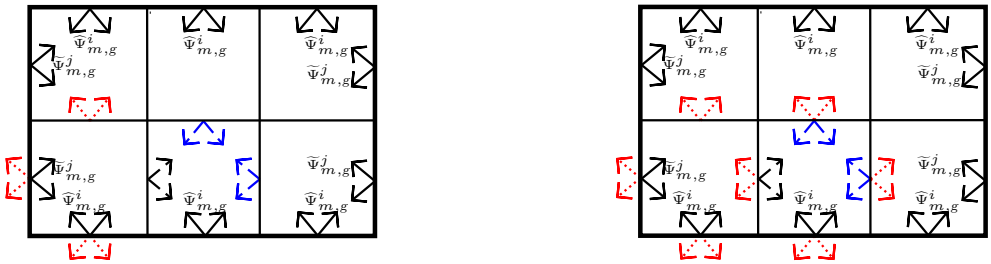

(a) Initial estimate

(b) Outgoing fluxes

Advancing from left to right of the initial $\Gamma_{i,j}$ node at the initial line, the Equations (25) and (26) are used to determine the α_ℓ parameters and the outgoing angular fluxes, $\widetilde{\psi}^j_{m,g}$

and $\widehat{\psi}^{i}_{m,g}$, at the interfaces of the remaining nodes. When the opposite end of the exit point is reached in the direction of x, in this case, it is switched to the next line in the direction of y and the movement starts again from left to right on the new line. The Equations (25) and (26) are still being used to determine the parameters α_ℓ, and the outgoing angular fluxes $\widetilde{\psi}_{m,g}$ and $\widehat{\psi}_{m,g}$ at the $\Gamma_{i,j}$ cells interfaces.

Figure 5: Incomming and Outgoing angular fluxes from the last node $\Gamma_{1,J}$ at the initial line

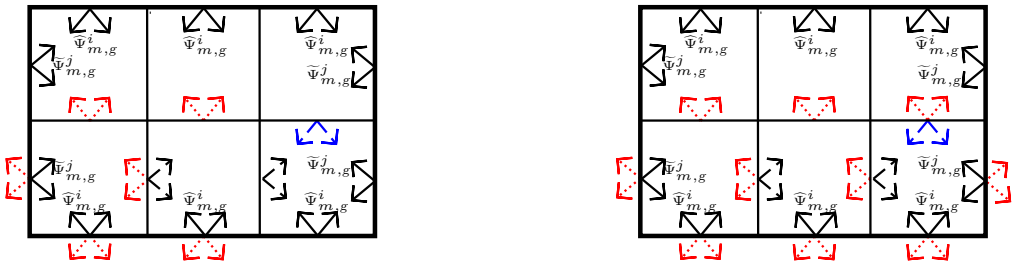

(a) Initial estimate

(b) Outgoing fluxes

When the opposite end is reached in the direction of x, it moves to the next line in the direction of y (Figure 6)

Figure 6: Incomming and Outgoing angular fluxes of the node $\Gamma_{i,j}$ in nwe row

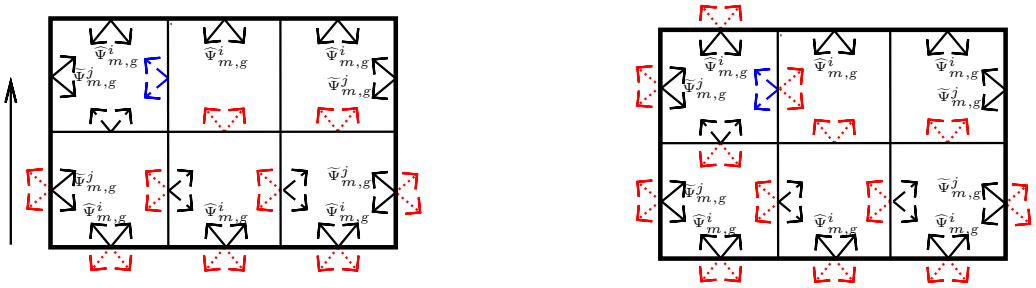

(a) Initial estimate

(b) Outgoing fluxes

The movement starts again from left to right on the new line(Figure 7). Equation (25) and (26) continue to be used to determine α_ℓ parameters and the outgoing $\widetilde{\psi}_{m,g}$ e $\widehat{\psi}_{m,g}$ angular fluxes at the cell interfaces $\Gamma_{i,j}$.

Finishing the calculations for all nodes in the grid, it is checked whether the stopping criterion is satisfied. This criterion establishes that the relative deviation between two consecutive estimates for the mean scalar flux at the energy groups on the node-edge does not exceed a pre-established ε positive value. If the stopping criterion is satisfied, the algorithm is terminated.

The updating of the transversal leakage terms and the particular solutions in each Γ_{ij} nodes is always carried out using the physical-material parameters of these nodes together with the boundary conditions and/or the estimates of the incoming angular fluxes at each one of these nodes. These estimates for the angular fluxes incoming on the nodes Γ_{ij} are constantly updated as the iterative process progresses.

Figure 7: Incomming and Outgoing angular fluxes at nodes $\Gamma_{i+1,\,j+1}$ in the new row

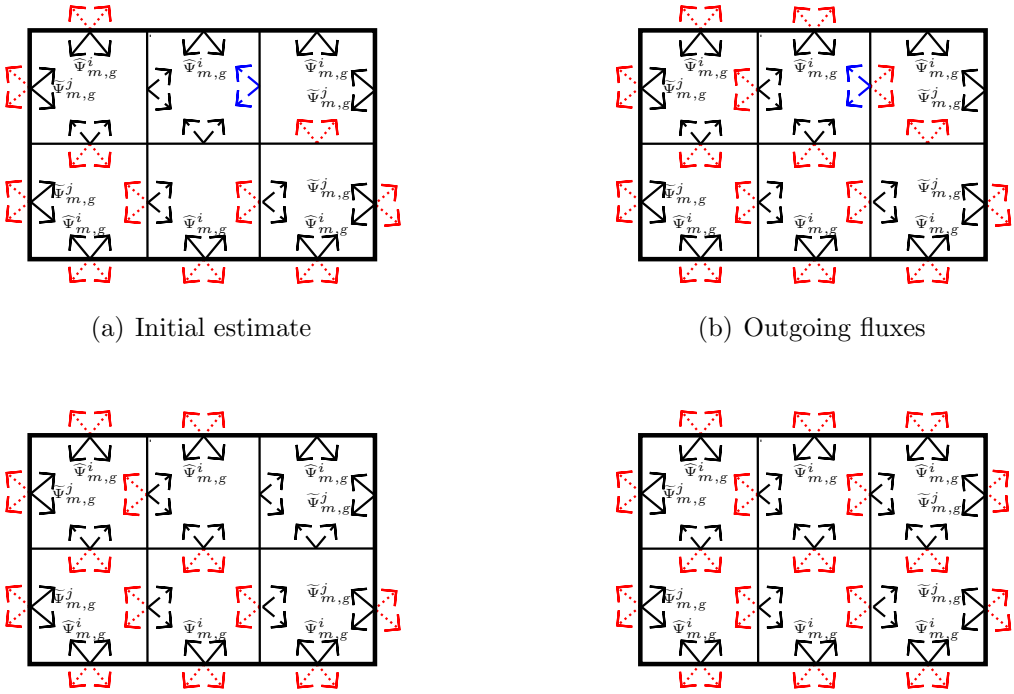

(a) Initial estimate

(b) Outgoing fluxes

(c) Initial estimate

(d) Outgoing fluxes

4. NUMERICAL RESULTS

In this section we examine two $X, Y-$ geometry model problems. The first is a heterogeneous domain developed by Barros and Larsen [4]. The results of the *SGF–CN* method are compared with the results obtained through the spectral nodal methodology *SDM–CN*.

This problem considers a 100 cm × 100 cm spatial domain with an isotropic unitary neutrons source, $Q_1 = 1$, at the center surrounded by a shielding material, $Q_2 = 0$, considering linearly anisotropic scattering [4]. The Figure 8 (not drawn to scale), presents a quarter of this configuration with the boundary conditions used to perform the simulation.

Tabel 1 lists the values of the physical-material parameters in each material zone.

Table 1: Physical - material parameters

Material Zone	$\sigma_T(cm^{-1})$	$\sigma_S^{(0)}(cm^{-1})$	$\sigma_S^{(1)}(cm^{-1})$
1	0.80	0.40	0.20
2	1.00	0.95	0.50

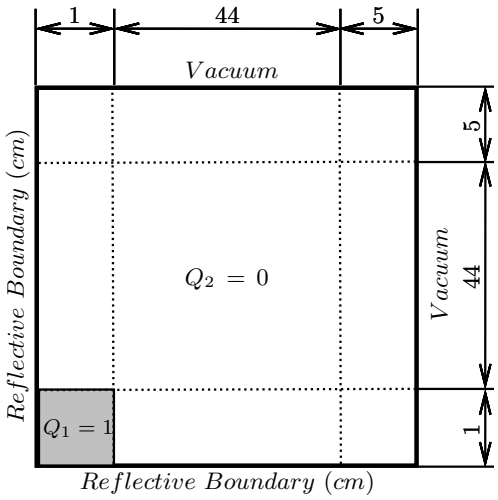

Figure 8: Model–problem 1.

The objective in this experiment is to determine the neutrons leakage through the right(R) and upper(U) boundaries of the domain represented in Fig. 8. The stopping criterion requires that the relative deviation between two consecutive estimates for the scalar flux on the faces of the domain nodes to be less than or equal to 10^{-7}.

The Table 2 is shown the numerical results of the right and upper boundary leakage calculations besides the relative deviations $\delta_U(\%)$ and $(\delta_R(\%))$ for the $SGF - CN$ and $SDM - CN$, using as reference the value obtained with the DD method using a $20 \times 880 \times 100$ nodes per region in the x and y direction. The DD method reaches the fine-mesh at 1000 nodes; which is the mesh size that for the scalar fluxes in the seventh decimal place do not have a significant variation.

To calculate the relative deviations $\delta(\%)$, in both cases, we use the expression

$$\delta(\%) = \left| \frac{S_{DD} - S_m}{S_{DD}} \right| \times 100, \tag{27}$$

where S_{DD} is the neutron leakage value obtained with the DD method used as a reference and S_m represents the neutron leakage value generated by each of the methods used to calculate such leakage in the specified boundaries.

As can be seen, in Table 2 the results obtained for the leaks in both boundaries are symmetrical and as the spatial grid becomes thinner, the results generated by both coarse mesh methods converge to the same result. The values for the relative percentage deviations of the methods $SGF - CN$ and $SDM - CN$ when comparing them with the DD method, present values less than 3 %.

The second model problem is a fixed source experiment in absorbing medium, which was suggested by the Argonne Code Center Benchmark Problems Committee and models a realistic shielding situation [13]. This problem has been designed to provide stringent tests for two-dimensional geometry transport codes with two energy groups [12].

Table 2: Neutrons leakage to Model Problem 1

$\Omega_x \times \Omega_y$ spatial grid	Method	Upper boundary leakage	$\delta_U(\%)^b$	Right boundary leakage	$\delta_R(\%)$
20x880x100	DD	4.99400E-06[c]	–	4.99400E-06	–
1x17x2	SGF-CN	4.88894E-06	2.1039	4.88894E-06	2.1039
	SDM-CN	5.13538E-06	2.8310	5.13538E-06	2.8310
1x26x3	SGF-CN	4.94060E-06	1.0693	4.94060E-06	1.0693
	SDM-CN	5.05927E-06	1.3070	5.05927E-06	1.3070
1x44x5	SGF-CN	4.97479E-06	0.3847	4.97479E-06	0.3847
	SDM-CN	4.97479E-06	0.3847	4.97479E-06	0.3847
2x88x10	SGF-CN	4.98905E-06	0.0991	4.98905E-06	0.0991
	SDM-CN	4.98905E-06	0.0991	4.98905E-06	0.0991

a. Neutrons leakage : $cm^{-2}\ s^{-1}$.
b. Relative deviations.
c. Read: 4.99400 x 10^{-6} .

The problem geometry is illustrated in Figure 9. The macroscopic cross sections for the homogeneous material of the system and the source density are listed in Table 3.

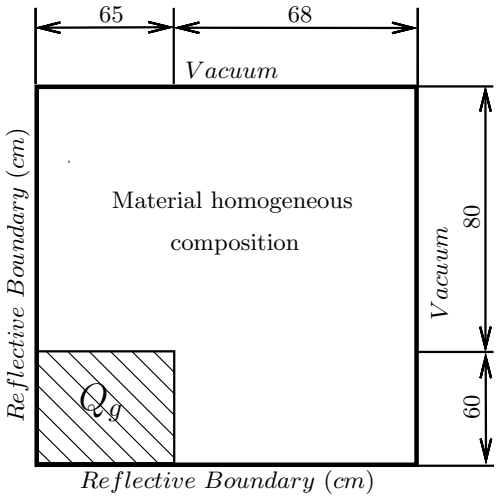

Figure 9: Model–problem 2.

To simulate this problem using the *SDM-CN* method, a spatial discretization grid it is defined as follows, in the direction of x, where it is the region with the uniform spatial source ($0 \leq x \leq 65$) was divided into 13 nodes and the region without source ($65 \leq x \leq 133$) into 14 nodes. Similarly, in the direction of the spatial variable y, it was divided into 12 nodes in the region with source ($0 \leq x \leq 60$) and 16 nodes in the region without source ($60 \leq x \leq 140$).

To compare the results obtained by the *SDM-CN* method, we use the reported results for this problem by Dias in [12], using the *DOT-II* and *TWOTRAN* codes together to

Table 3: Macroscopic Cross Sections (cm^{-1}) and source density ($neutrons/cm^3$) for the second model problem

	$g=1$	$g=2$
σ_{T_g}	0.092104	0.100877
Q_g	0.006546	0.017701
	$\sigma^{(0)}_{s_{g'\to g}}$ (cm^{-1})	
$g'=1$	0.006947	0.023434
$g'=2$	0.000000	0.004850

the results of the *SGF-CN* method reported by Menezes [13]. The Table 4 shows the numerical results obtained for the total leakage for both energy groups, $J_+^{T_g}$, at the right boundary of the system shown in Figure 9. The results listed in [12] for code *TWOTRAN* considering a spatial discretization grid of 6804 nodes, $(39 \times 42) \times (36 \times 48)$, were used as reference for calculating the relative relative deviation of all methods addressed in this experiment using a spatial discretization grid of 756 nodes, $(13 \times 14) \times (12 \times 16)$. Were considered S_8 and S_{12} sets of the Level Symmetric Quadrature, LQ_N.

Table 4: Neutron leakage [a] by right boundary

			$J_+^{T_g}$			
S_N	g	Fine mesh reference	*TWOTRAN*	$DOT-II$	$SGF-CN$	$SDM-CN$
8	1	5.7400E-04[b]	5.0000E-04 (12.8920 %)[c]	4.9900E-04 (13.0662 %)	5.4744E-04 (4.6272 %)	5.4744E-04 (4.6279 %)
	2	9.2100E-04	8.0000E-04 (13.1379 %)	7.7500E-04 (15.8523 %)	8.7832E-04 (4.6341 %)	8.7832E-04 (4.6346 %)
12	1	5.5700E-04	4.9600E-04 (10.9515 %)	4.9900E-04 (10.4129 %)	5.4833E-04 (1.5566 %)	5.5360E-04 (0.6110 %)
	2	8.9100E-04	7.7600E-04 (12.9068 %)	7.7500E-04 (13.0191 %)	8.7868E-04 (1.3827 %)	8.9028E-04 (0.0806 %)

a. Neutrons leakage : $\mathrm{cm}^{-2}\ \mathrm{s}^{-1}$,
b. Read: 5.7400 x 10^{-4},
c. Percent relative deviation .

As can be seen in Table 4, the relative percentage deviations of the results generated by the *SDM-CN* method for the right boundary leakage were always smaller than the relative deviations generated by the *DOT–II* and *TWOTRAN* similar to the behavior of the *SGF–CN* method. It may also be noted that the relative percent deviations of the method results in the SDM-CN method decreased with increasing quadrature of the symmetry level.

5. CONCLUSIONS

In this paper, an analytical $X, Y-$ geometry coarse-mesh numerical method, $SDM-CN$, for multigroup fixed source linearly anisotropic S_N problem in slab geometry has been

described and developed. The multigroup $SDM - CN$ discretization scheme preserves the general analytic solution of the multigroup S_N equation in each spatial node, converges to numerical results that are continuous across each node interface and satisfies the external boundary conditions whether the mesh size order or quadrature set used. The $SDM - CN$ method converges to numerical solutions ,that are free from spatial truncation errors because their results coincide with the numerical results obtained from the analytic solution of the analyzed S_N problem regardless the definition of the spatial grid or the angular quadrature used, same as the $SGF - CN$ method while the fine-mesh DD method, *DOT–II* and *TWOTRAN* solution are not. When calculating the transverse leakage terms, in the method *SDM–CN*, these are approximated by constants. These relative deviations can be attenuated if a better approximation is made for the transverse leakage terms. We plan to report on the analytic–numerical method results after they have been implemented and thoroughly tested.

ACKNOWLEDGMENTS

In memory of professor Marcos Pimenta de Abreu. This study was financed in part by the Coordenação de Aperfeiçoamento de Pessoal de Nível Superior - Brasil (CAPES) - Finance Code 001.

REFERENCES

1. Duderstadt, J. J. and Martin, W. R., *Transport Theory*, Wiley–Interscience, New York, USA (1979)
2. E. E. Lewis, and W. F.Miller, *Computational methods of neutron transport*, American Nuclear Society, Illinois, USA (1993).
3. Oliva, A. M. and Alves Filho, H. and Silva, D. J. and García, C. R., The spectral nodal method applied to multigroup S_N neutron transport problems in one–dimensional geometry with fixed–source, *Progress in Nuclear Energy*, **22**, pp. 106-113, (2018).
4. R.C. Barros and E.W. Larsen , "A Spectral Nodal Method for One-Group X, Y-Geometry Discrete Ordinates Problems", *Nuclear Science and Engineering*, **111**, pp. 34–45, (1992).
5. Barros, R.C. and Larsen, E.W., A Numerical Method for Multigroup Slab-Geometry Discrete Ordinates Problems with no Spatial Truncation Error, *Transport Theory and Statistical Physics*, **20**,pp. 441–462, (1991).
6. Case, K.M. and Zweifel, P.F., Linear Transport Theory, Addison-Wesley, Reading, Massachusetts (1967).
7. Oliva,A. M., Método Espectral Determinístico para a solução de problemas de transporte de nêutrons usando a formulação das ordenadas discretas, D.Sc. dissertation, IPRJ/UERJ, Nova Friburgo, RJ, Brasil, 2018.
8. Menezes, W.A. and Filho, H. A. and Barros, R.C., Spectral Green's function nodal method for multigroup S_N problems with anisotropic scattering in slab-geometry non-multiplying media, *Annals of Nuclear Energy*, **64**, pp. 270–275, (2014).

9. R.C. Barros , A Spectral Nodal Method for the Solution of Discrete Ordinates Problems in one and two Dimensional Cartesian Geometry, Ph.D. dissertation, The University of Michigan, Ann Arbor, Michigan, 1990.
10. M. P. de Abreu, Métodos Determinísticos Livres de Aproximações Espaciais para a Solução Numérica Dominante de Problemas de Autovalor Multiplicativo na Formulação de Ordenadas Discretas da Teoria do Transporte de Nêutrons, D.Sc. dissertation, COPPE/UFRJ, Rio de Janeiro, RJ, Brasil, 1996.
11. Otto, A. C., Estudo e aplicação dos códigos ANISN e DOT 3.5 a problemas de blindagem de radiações nucleares, Masters Thesis, IPEN/CNEN, Universidade de São Paulo, SP, Brasil, 1983.
12. Dias, A. F., Estudo e aplicação dos códigos ANISN e DOT–II em problemas de física de reatores, Masters Thesis, IPEN/CNEN, Universidade de São Paulo, SP, Brasil, 1980.
13. Menezes,W. A., Métodos espectronodais para cálculos de partículas neutras com fonte fixa na formulação de ordenadas discretas e multigrupo de energia., D.Sc. dissertation, IPRJ/UERJ, Nova Friburgo, RJ, Brasil, 2012.